

EVAPORATION-DRIVEN NANOMACHINING TO FABRICATE NANOPORES IN SiO₂

L.J. de Vreede^{1,2*} A. van den Berg^{1,2} and J.C.T Eijkel^{1,2}

¹MESA+ Institute for Nanotechnology, University of Twente, the Netherlands and

²MIRA Institute for Biomedical technology and Technical Medicine, University of Twente, the Netherlands

ABSTRACT

We demonstrate a novel method to produce high aspect ratio nanopores in fused silica (SiO₂) using basic cleanroom techniques and high temperature. We found that gold nanoparticles on silicon oxide (SiO₂) move perpendicularly to the surface into the substrate when heated at 1050°C, creating cylindrical nanopores that can reach extreme aspect ratios (diameter \cong 25 nm, length up to 800 nm). Fabrication of single nanopores as well as of freely patterned nanopore arrays is straightforward by prior Au surface patterning without the need for conventional nanolithographic techniques. We demonstrate manufacturing of arrays of 10⁶ dead-end pores and manufacturing of membrane through-holes.

KEYWORDS: Gold Nanoparticle, Silica, Solid-State Nanopore, Membrane

INTRODUCTION

Closed-end pores are for example useful as a mold for atomic force microscope (AFM) tips. Machined as through holes, nanopore arrays or single pores are of great practical use for applications in high-throughput DNA sequencing, molecular sensing and molecular separations. An array of 10⁶ circular gold patches of 18 nm thickness and 1 μ m diameter on a substrate of fused silica glass (SiO₂) was heated for several hours at 1050°C. After initial dewetting, hexagonal Au nanocrystals formed that became surrounded by an increasingly thick and high silica ridge from which a Au bulge protruded (Fig. 1a). The Au particles then moved into the SiO₂ (Fig. 1b and Fig. 2a) at a velocity of \sim 100 nm/hr while remaining connected to the substrate surface by a nanopore as shown in Figs. 1c,d. Experiments at 1050°C with the gold facing up and down showed a similar penetration, ruling out an influence of gravity.

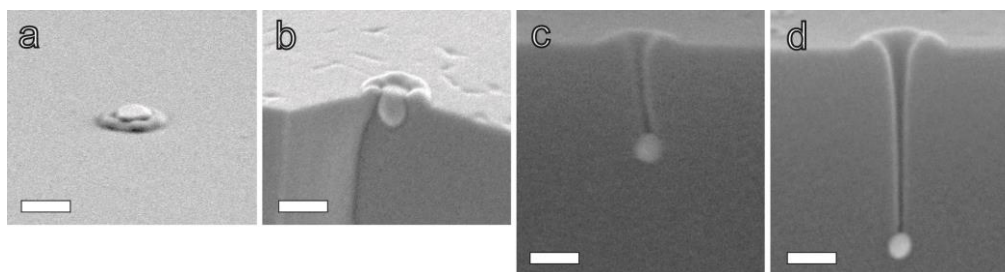


Figure 1: high resolution scanning electron microscope (HRSEM) pictures at four stages of heat treatments. (a) formation of a SiO₂ ridge and gold cap after 36 hours at 900°C, (b) Gold nanoparticle (GNP) penetrating into the fused silica after 10 minutes at 1050°C and (c) GNP penetration into the glass and pore formation after 1 hour at 1050°C (d) penetration after 3 hours at 1050°C. Scale bars represent 100nm. Figures (b-d) were produced after fracturing the substrate.

THEORY

The creation of nanopores is explained by dissolution of the ceramic along the interface with the metal and transport of ceramic to the air/particle/ceramic triple line where it precipitates, allowing the system to remodel around the triple line to minimize the total interfacial energy. [1,2] Energy at the triple line is

minimized when the Smith equation is satisfied stating $\frac{\gamma_{AG}}{\sin \theta_S} = \frac{\gamma_{AS}}{\sin \theta_G} = \frac{\gamma_{SG}}{\sin \theta_A}$, where γ is the interfacial energy (J/m^2) and θ the angle occupied by the respective phases – here air (A), SiO_2 (S) and gold (G). [3] We will argue that the structures observed by us can be explained by continuous maintenance of local equilibrium at the triple line in combination with a continuous evaporation of the GNP Au, where the latter is well documented at these temperatures. [4] It should thereby be kept in mind that *local* triple-line equilibrium together with Au evaporation can explain the structures obtained, but that they do not represent *global* equilibrium since only the ceramic in the Au/ SiO_2 interface is mobile. Thus the growth of nanopores with large surface-area can result from this process.

EXPERIMENTAL

We observed the formation of nanopores up to a depth of 840 nm and a final diameter of approximately 25 nm, see figure 2a after 9 hours of heating at 1050°C . Figure 2b shows the nanopore length over time for the 1050°C heat treatment. Electron microscopy pictures of the system did not show any morphologic differences between the bulk SiO_2 and the SiO_2 surrounding the pore and local X-ray spectroscopy showed no evidence of Au diffusion into the SiO_2 . The process has also been carried out on a thin SiO_2 film in order to obtain nanopore through holes. Creating pores with a diameter of 50 nm.

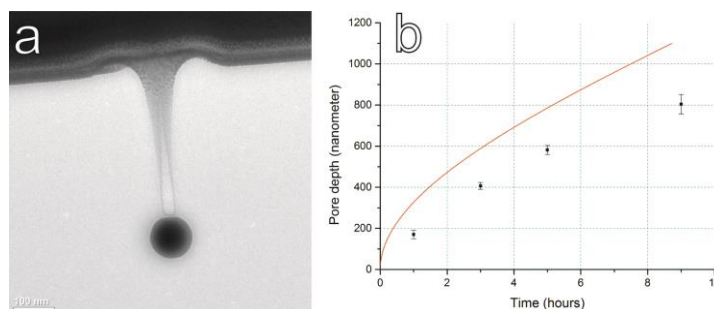


Figure 2: Pore formation over time. (a) A STEM cross-section of a structure formed after 3 hours at 1050°C . On top it shows the ridge surrounding the nanopore entrance and at the bottom the GNP. (b) In black the measured nanopore length versus heating time at 1050°C . Error bars represent standard deviation with $n = 6$.

RESULTS AND DISCUSSION

The proposed mechanism is schematically shown in Fig. 3 and can be related to Figs. 1a-d and Fig. 2a. Substituting the interfacial energies [5,6,7] in the Smith equation yields an equilibrium Au angle θ_G at the triple line of 167° , SiO_2 angle θ_S of 103° and air angle θ_A of 90° . The Au initially forms a slight bulge (Figs. 1a,b and Fig. 4), in accordance with the $\theta_A \approx 90^\circ$ satisfying the Smith equation. In course of time, continued Au evaporation and SiO_2 transport from below the GNP cause the GNP to move into the SiO_2 . To satisfy the Smith equation for an embedded GNP, the triple line moves to the top of the particle, narrowing the pore formed. On deeper embedding the triple line does not close, since this would imply a Au angle θ_G of 180° . Application of the Smith equation instead yields that the triple line position must be at the edge of a pore of radius $d \sin(\theta_G)$ for a spherical GNP of diameter d (Fig. 3g). Pore diameter d_p at this stage becomes linearly dependent on the pore length with the pore narrowing rate equalling $d(d_p)/dy = -3/2\sin^3(\theta_G)$, where y is the surface-normal coordinate. Via this mechanism, the Au progressively moves into the SiO_2 , leaving a pore with a volume equal to the evaporated volume of Au and a narrowing diameter due to the decrease in d .

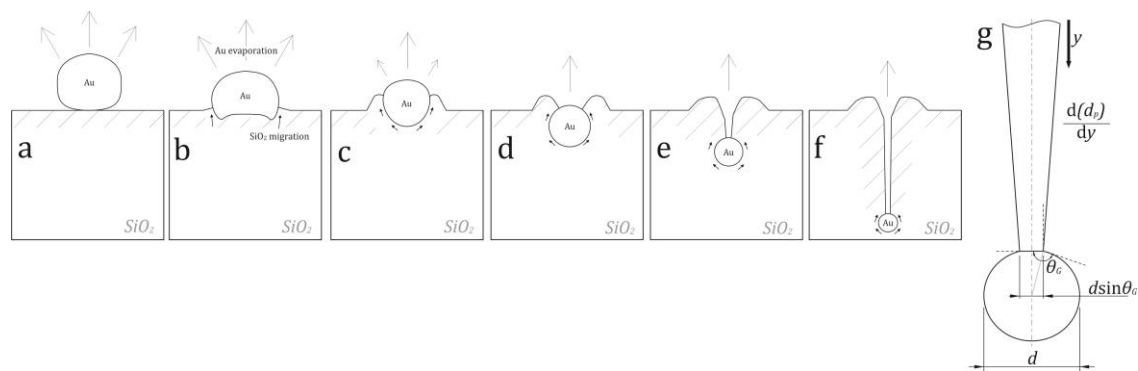


Figure 3: A cross-sectional schematic representation of the pore formation process at 1050°C. a) Gold dewetting, directly followed by b-c) ridging of SiO₂. d-f) Continuous Au evaporation and transport of SiO₂ along the SiO₂/Au interface to the triple line creates an increasingly narrow pore facing into the substrate. g) At the pore end the triple line is positioned on the GNP surface where the Au angle θ_G equals its equilibrium value of 167°. Now the relation between particle diameter d and pore diameter $d_p = d \sin \theta_G$. Pore narrowing rate with depth y is given by $d(d_p)/dy = -3/2 \sin^3(\theta_G)$.

CONCLUSION

We present a new nanopore manufacturing method. Any metal/ceramic combination with a metal angle slightly smaller than 180° where the metal promotes surface diffusion of the ceramic and where no reactions between metal and ceramic or metal and atmosphere take place, will be suitable for this machining method.

ACKNOWLEDGEMENTS

Financial support by STW and NanoNextNL are gratefully acknowledged.

REFERENCES

- ¹ Saiz, E.; Cannon, R.M.; Tomsia, A.P.; *Reactive Spreading in Ceramic/Metal Systems*, Oil Gas Sci. Technol. Rev. IFP, **56**, 89-96 (2001)
- ² Fyfe, W. S.; Turner F.J.; Verhoogen J., *Metamorphic Reactions and Metamorphic Facies*, (The Geological Society of America, Memoir 73, New York, 1958).
- ³ Rohrer, G.S., “*Introduction to Grains, Phases, and Interfaces—an Interpretation of Microstructure,*” Trans. AIME, 1948, vol. 175, pp. 15–51, by C.S. Smith”, Metallurgical Mater. Trans. A, **41A**, 1063 (2010)
- ⁴ Meng, G.; et al. *Pressure-induced evaporation dynamics of gold nanoparticles on oxide substrate*, Phys. Rev. E **87**, 012405 (2013)
- ⁵ Ricci, E.; Novakovic, R.; *Wetting and surface Tension Measurements on Gold alloys*. Gold Bull. **34**, 41 (2001)
- ⁶ Ruffino, F.; et al., *Thermodynamic Properties of Supported and Embedded Metallic Nanocrystals: Gold on/in SiO₂*. Nanoscale Res. Lett. **3**, 454-460 (2008)
- ⁷ Brunauer, S.; Kantro, D.L.; Weise, C.H.; *The surface energies of amorphous silica and hydrous amorphous silica*. Can. J. Chem. **34**, 1483-1496 (1956)

CONTACT

* L.J. de Vreede; phone: +31-53-489-9433; l.j.devreede@utwente.nl